η PHOTOPRODUCTION FROM DEUTERON AT E_γ=0.7÷1.5 GeV

O. Bartalini[1,2], V. Bellini[3,4], J.P. Bocquet[5], M. Capogni[1,2], M. Casano[2], M. Castoldi[6], P. Calvat[5], A. D'Angelo[1,2], J.-P. Didelez[7], R. Di Salvo[1], A. Fantini[1,2], G. Gervino[8], F. Ghio[9], B. Girolami[9], M. Guidal[7], A. Giusa[3,10], E. Hourany[7], R. Kunne[7], V. Kouznetsov[11], A. Lapik[11], P. Levi Sandri[12], A. Lleres[5], D. Moricciani[1,2], A. Mushkarenkov[11], V. Nedorezov[11], L. Nicoletti[2], C. Perrin[5], D. Rebreyend[5], F. Renard[5], N. Rudnev[11], T. Russew[5], G. Russo[10], C. Schaerf[1,2], M.-L. Sperduto[3,10], M.-C. Sutera[10], A. Turinge[11]

[1] *Università di Roma "Tor Vergata", I-00133 Roma, Italy*

[2] *INFN Sezione di Roma "Tor Vergata", I-00133 Roma, Italy*

[3] *Università di Catania, I-95123 Catania, Italy*

[4] *INFN Laboratori Nazionali del Sud, I-95123 Catania, Italy*

[5] *IN2P3, Laboratoire de Physique Subatomique et de Cosmologie, 38026 Grenoble, France*

[6] *INFN Sezione di Genova, I-16146 Genova, Italy*

[7] *IN2P3, Institut de Physique Nucléaire d'Orsay, 91406 Orsay, France*

[8] *INFN Sezione di Torino, I-10125 Torino, Italy*

[9] *INFN Sezione di Roma I, I-00185 Roma, Italy*

[10] *INFN Sezione di Catania, I-95123 Catania, Italy*

[11] *Institute for Nuclear Research, 117312 Moscow, Russia*

[12] *INFN Laboratori Nazionali di Frascati, I-00044 Frascati, Italy*

Abstract

The preliminary results obtained in the GRAAL experiment on exclusive η-mesons photoproduction on the quasi-free proton and neutron are reported. Comparison with the MAID calculations and results of other experiments are presented.

1 Introduction

Study of η-mesons photoproduction on nucleon is particularly suitable due to isospin conservation in final state which selects resonances with isospin 1/2 only. Moreover, study of these reactions on neutron in conjunction with proton data provides information about isospin dependence of photoexcitation amplitudes. Deuteron is a most suitable neutron target for such study and it also opens possibility to study nuclear effects. Extensive studies of η-mesons photoproduction at $E_\gamma < 1$ GeV revealed strong dominance of S11(1535) resonance. (See [1, 2, 3] and reference therein). This result can be quite well explained by the MAID

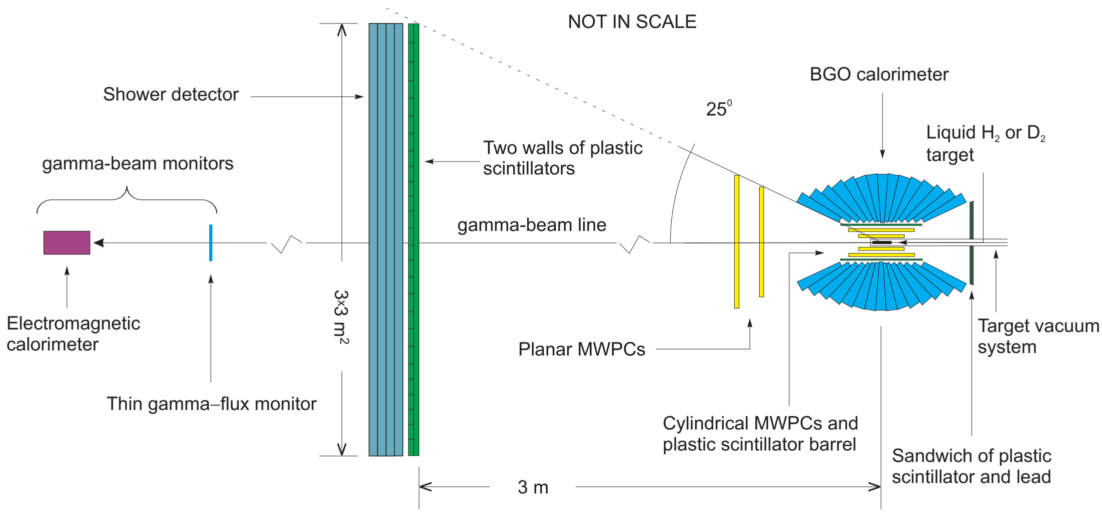

Fig. 1: Sketch of the GRAAL detection system.

analysis [4]. Recently, the energy region was extended for $E_\gamma > 1$ GeV [5, 6]. As well, the GRAAL and TAPSCB-ELSA collaborations reported the preliminary results on the beam asymmetry [7, 8] and the cross-sections [8] of η-mesons photoproduction on neutron (quasi-free from deuteron). The result from TAPSCB-ELSA experiment shows a bump structure in the neutron cross-section around the total c.m. energy $W = 1.675$ GeV which is not seen in the proton cross-section. At present time, this result is extensively discussed [9, 10]. There are two models which can qualitatively explain the neutron cross-section. First one is Isobar Model [11] which is used in the MAID calculations. This model explains the experimental result by the contribution of D15(1675) resonance imposing branching ratio $\Gamma_{\eta N}/\Gamma_{tot} = 17\%$. Alternatively, as it is suggested in work [12], the Chiral Soliton Model can also explain the neutron data by contribution of the narrow P11 resonance with mass around 1.7 GeV.

In the present work the preliminary results on the differential and total cross-sections of η-mesons photoproduction on the quasi-free proton and the quasi-free neutron at $E_\gamma = 0.7 \div 1.5$ GeV are reported. The data were obtained in the GRAAL experiment [13] with the use of a liquid deuterium target.

2 The setup

The beam of polarized tagged photons is produced by the backscattering of laser light on the 6.04 GeV electrons circulating in the storage ring of the ESRF (Grenoble, France). When using the green 514 nm and the ultraviolet 351 nm laser lines, the tagged spectrum covers the energy range 0.55÷1.5 GeV. The tagging detector provides an energy resolution of 16 MeV(FWHM).

The detection system (Fig. 1) includes three main parts.

- The forward part in the angular range of $\theta \leq 25^\circ$ which is covered by:

  1. two planar wire chambers for the tracking of charged particles;
  2. two walls of plastic scintillators consisting of 26 horizontal and 26 vertical bars, placed at 3 m from the target (They are designed for TOF, dE/dx, and angu-

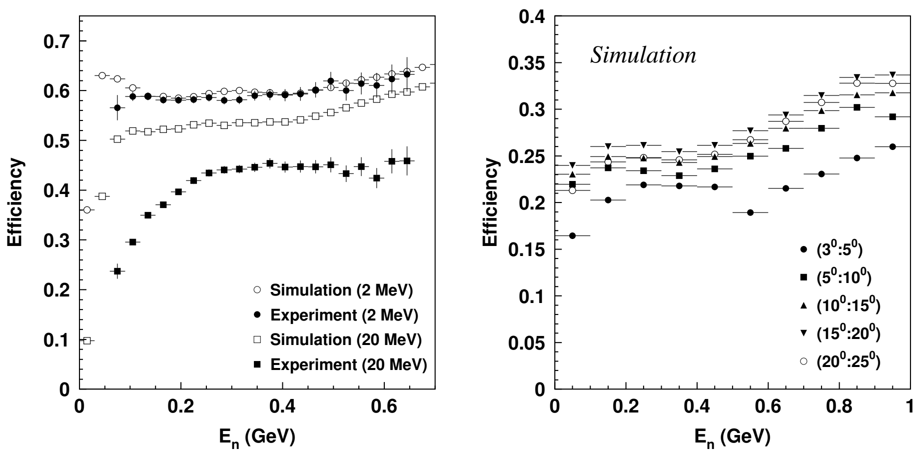

Fig. 2: The neutron detection efficiency in the BGO calorimeter (left) and the shower detector (right). See text for detailed explanation.

lar measurements of charged particles, as well as for particle identification and discrimination.);

3. the shower detector consisting of 16 vertical modules made of lead and plastic scintillator [14] (It provides TOF, dE/dx, and angular measurements, as well as the identification of both neutral (γ, neutron) and charged particles.);

- The central part, covering the angular range $25° \leq \theta \leq 155°$, which consists of:

  1. two cylindrical wire chambers for the tracking of charged particles;
  2. the barrel made of 5-mm-thick plastic scintillator bars for dE/dx measurement and the discrimination and identification of charged particles;
  3. the electromagnetic calorimeter made of 480 BGO crystals [15] (It is designed to measure energies and angles of gammas and low-energy protons up to 300 MeV/c, as well as the angles and ΔE response for charged pions and neutrons);

- The backward part within the angular range of $\theta \geq 155°$, which is covered by two plastic scintillator disks separated by a 1-cm-thick lead converter, which are sensitive to both neutral and charged particles (It is used as a veto detector).

The gamma-beam monitors are used in the determination of the γ-flux.

3 Neutron detection efficiency

The neutron detection efficiency was studied in simulation (with the GEANT3.21 package) and experiment for BGO calorimeter [15] and was simulated for the shower detector. Fig. 2 shows the neutron detection efficiency as a function of the neutron kinetic energy ((left) and (right) correspond to the BGO calorimeter and the shower detector, respectively). It was obtained a good agreement between the simulated and experimental data for a low (2 MeV) energy threshold of the BGO clusters (group of fired crystals) while for higher energy threshold (20MeV) there is discrepancy. Also, it was not obtained an angular dependence of the BGO efficiency. The simulated neutron detection efficiency of the shower detector

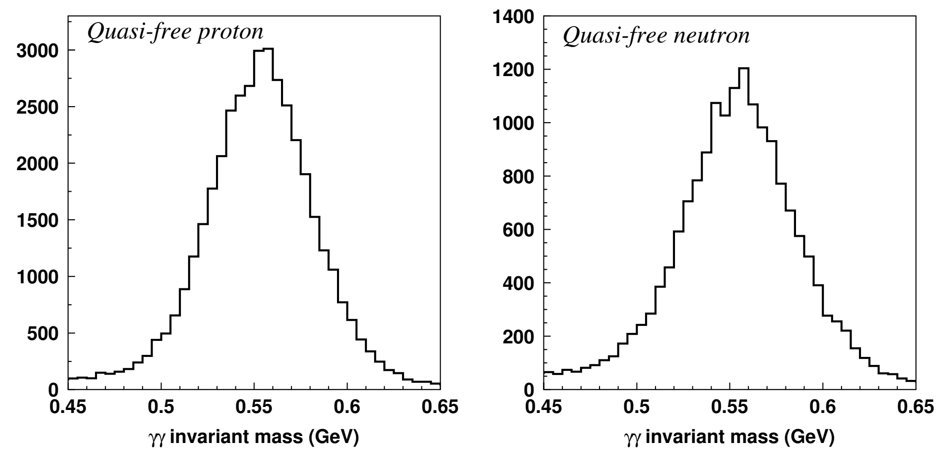

Fig. 3: Invariant mass of 2γ from η-mesons decay.

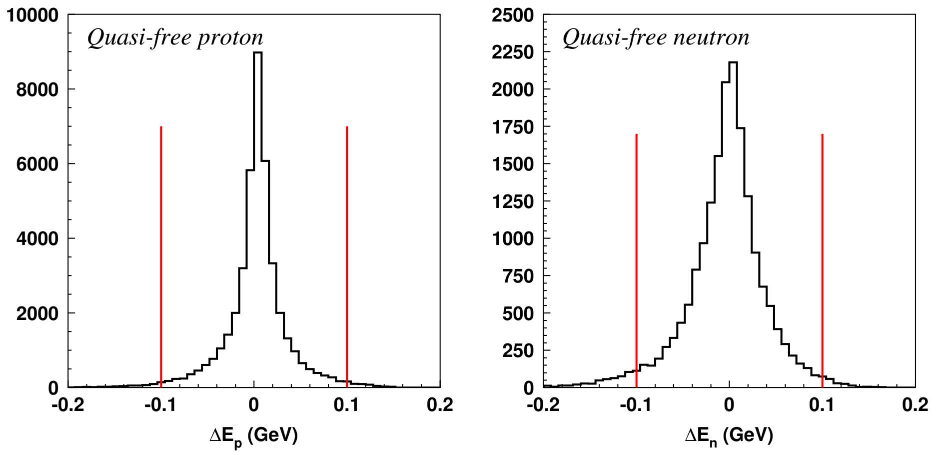

Fig. 4: Distributions of the difference between measured and expected energies of the recoil nucleons in the ηN c.m. frame.

is about twenty-five percents on average. Also it was obtained an angular dependence of this efficiency. Experimental study of the shower detector response for neutrons was not still done. Nevertheless, the information from this detector was used in the present analysis taking into account the simulated efficiency.

4 Event selection

In the present experiment two gammas from η decay and recoil nucleon (proton or neutron) were detected in coincidence. The η-mesons were identified via the standard invariant mass analysis of the two detected gammas (Fig. 3). Then, events which satisfy to the two-body kinematics of the quasi-free reactions, were selected via the missing energy analysis (Fig. 4), as well as the angles balance (Figs. 5 and 6).

The kinematic over-determination allows us to reconstruct the total c.m. energy W of the ηN system and to deduce the effective incident γ energy E^*_γ which is corresponded to

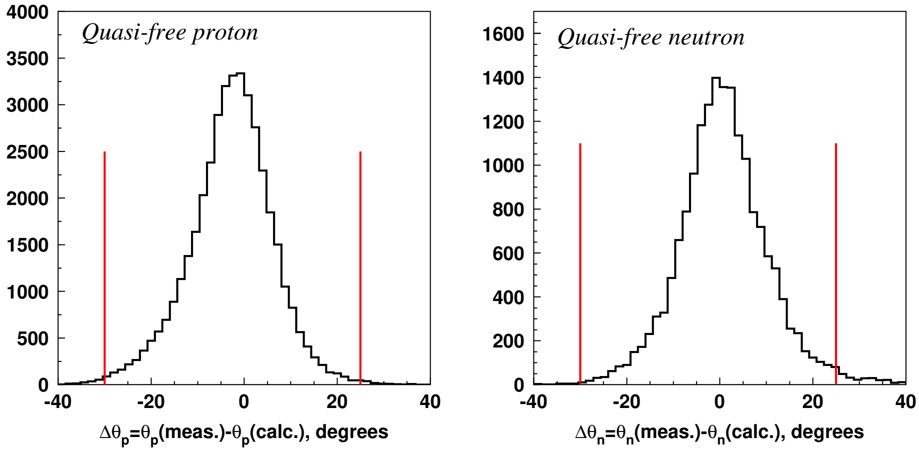

Fig. 5: The balance of the recoil nucleon polar angle.

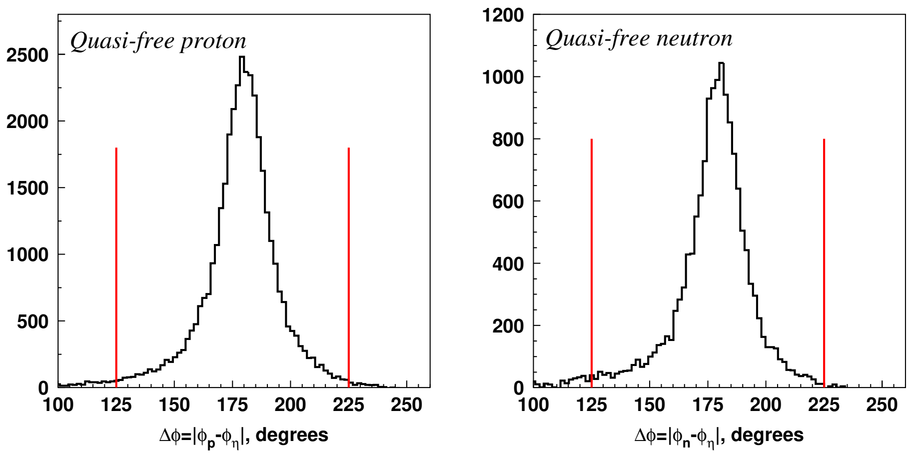

Fig. 6: The balance of the azimuthal angles.

the same c.m. energy for an target nucleon at rest:

$$W^2 = (E_\eta + E_N)^2 - (\vec{p}_\eta + \vec{p}_N)^2, \tag{1}$$

$$E^*_\gamma = \frac{W^2 - m_N^2}{2m_N}, \tag{2}$$

where E_η and $\vec{p}_\eta$ are the detected energy and momentum of η-meson, E_N and $\vec{p}_N$ are the recoil nucleon energy and momentum which are deduced from energy of the incident γ and E_η, m_N is mass of the recoil nucleon. In this way the Fermi smearing is eliminated from energy dependence of the cross-sections. As well, the cm polar angle θ^{cm} was calculated taking into account the Fermi momentum of target nucleon.

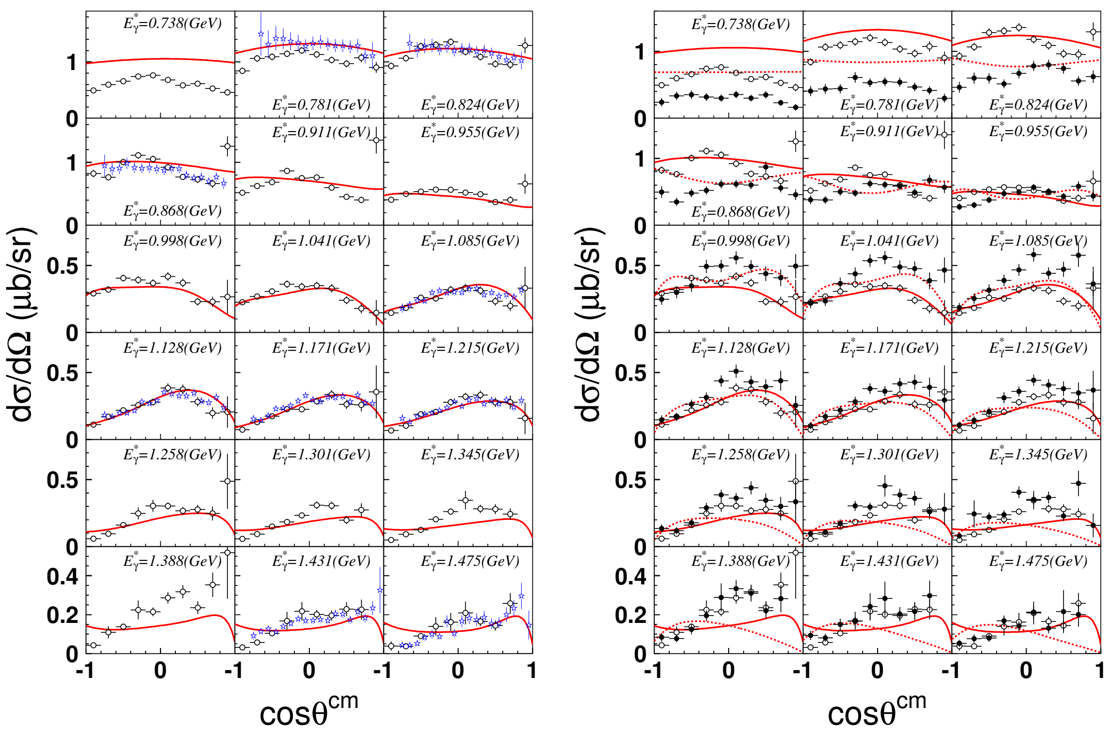

Fig. 7: The differential cross-sections of the η-mesons photproduction on the quasi-free proton (open circles) and the quasi-free neutron (full circles) in comparison with ETA-MAID2001 [4] predictions (solid and dashed lines correspond to $\gamma p \rightarrow \eta p$ and $\gamma n \rightarrow \eta n$, respectively). Stars show the data obtained in work [5] on free proton.

5 Results

5.1 Angular distributions

The differential cross-sections of the reaction $\gamma d \rightarrow \eta pn(spectator)$ are shown by circles on Fig. 7(left) as a function of $cos\theta_{\eta}^{cm}$. The data obtained in experiment CB-ELSA [5] on free proton as well as MAID calculations [4] are plotted for comparison by stars and solid line, respectively. One can see the data for free and quasi-free proton are in close agreement. Influence of the nuclear effects (e.g. FSI) seems to be negligible. It can indicate on the possibilities to extract the neutron data from the measurement on deuteron target without additional corrections. Also, it is seen that behavior of the angular distributions obtained in experiment and predicted by MAID are different at $E_{\gamma} > 1.25$ GeV.

The differential cross-sections of the reaction $\gamma d \rightarrow \eta np(spectator)$ are shown by filled circles on Fig. 7(right) in comparison with the data for the reaction $\gamma d \rightarrow \eta pn(spectator)$ as well as MAID predictions. One can see that the angular distribution in case of quasi-free proton and quasi-free neutron are different up to $E_{\gamma} \sim 1.13$ GeV. At higher energy, behavior of these angular distributions become very similar to each other. Additionally, the angular distributions of η photoproduction on quasi-free neutron poorly agree with MAID predictions.

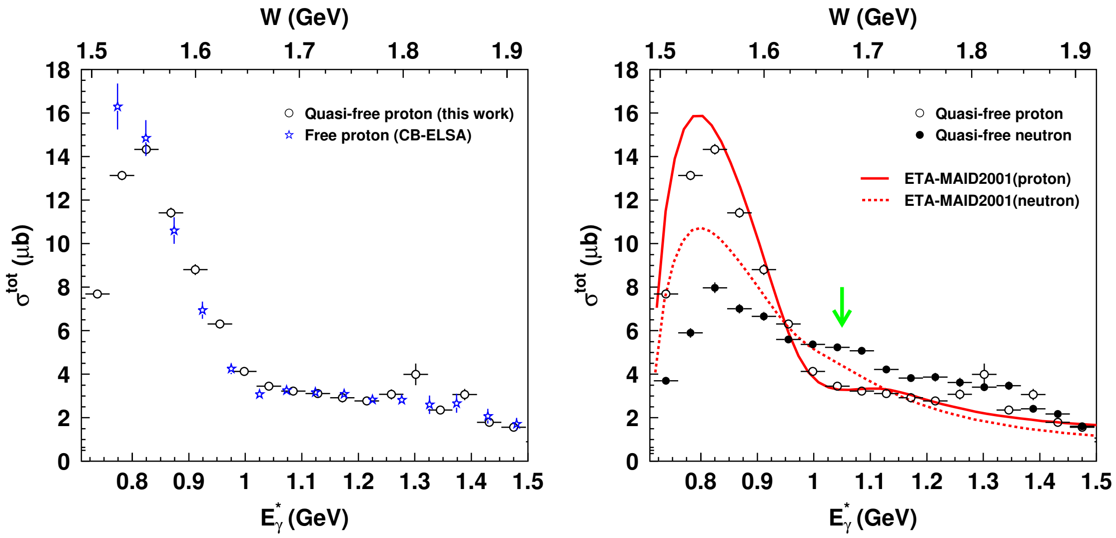

Fig. 8: The total cross-sections of η-meson photproduction on quasi-free proton and quasi-free neutron. All notations are identical to Fig. 7.

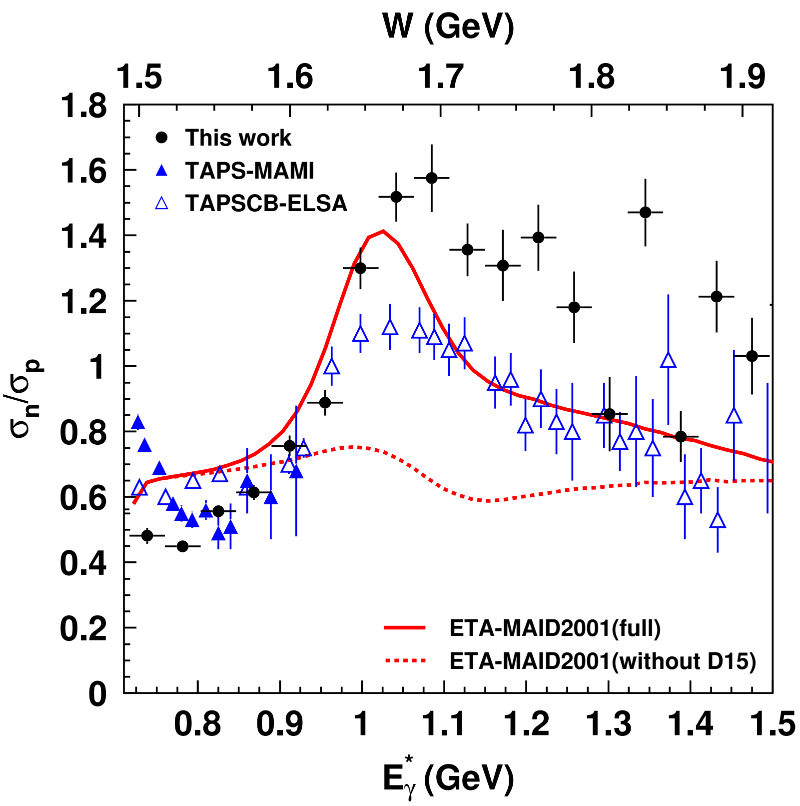

Fig. 9: The neutron/proton cross-sections ratio obtained in the present work (full circles) in comparison with TAPS-MAMI [1] (full triangles) and TAPSCB-ELSA [8] (open triangles) results. Solid line shows the calculation of the full MAID model, while the dashed line corresponds to the MAID calculation without the D15(1675) resonance contribution.

5.2 Total cross sections

The total cross-sections of η-meson photproduction on quasi-free proton and quasi-free neutron are shown on Figs. 8(left) and 8(right), respectively. All notations are identical to Fig. 7. Much as the differential cross-sections, the total cross-section on quasi-free proton is in good agreement with both the CB-ELSA data and MAID calculation for $E_\gamma < 1.25$ GeV. The difference seen at $E_\gamma \sim 0.740$ GeV is due to a systematic uncertainty, presumably.In case of the quasi-free neutron (Fig. 8(right)), the total cross-section has poorly agreement with respective MAID predictions. Moreover, the total cross-sections on quasi-free proton and quasi-free neutron have an opposite behavior in the region around $E_\gamma \sim 1.05$ GeV. The similar result was obtained in the TAPSCB-ELSA experiment [8].

Fig. 9 shows a ratio of the obtained total cross-sections σ_n/σ_p in comparison with the results from the previous experiments and MAID calculations. As it is seen, the MAID model qualitatively explains behavior the retion σ_n/σ_p. The restricted MAID calculations, in which the D15(1675) resonance is excluded, shows the important role of the D15(1675) resonance in the η-meson photoproduction on the neutron.

6 Summary

The preliminary results on exclusive η-mesons photoproduction on the quasi-free proton and neutron were reported. It was obtained close agreement between the quasi-free proton data and free proton data obtained earlier. At the same time, both these data are in disagreement with MAID prediction at $E_\gamma > 1.25$ GeV. The angular distributions of η photoproduction on the proton and neutron targets are different up to $E_\gamma \sim 1.13$ GeV and become very similar to each other at the higher energies. Additionally, the angular distributions of η photoproduction on quasi-free neutron poorly agree with MAID predictions. The neutron/proton cross-section ratio shows a rise up to ~ 1.5 at $E_\gamma \sim 1.05$ GeV. Behavior of the neutron/proton cross-section ratio agrees with results obtained earlier in the different experiments and can be qualitatively explained by the MAID analysis.

This work was supported by RFBR, grant no. 04-02-16996-a.

References

[1] J. Weiß et al., Eur. Phys. J. A 16, 275 (2003).

[2] F. Renard et al., Phys. Lett. B 528, 215 (2002).

[3] B. Krusche et al., Phys. Rev. Lett. 74, 3736 (1995).

[4] http://www.kph.uni-mainz.de/MAID/eta/etamaid.html

[5] V. Credé et al. Phys. Rev. Lett. 94, 012004 (2005).

[6] M. Dugger et al., Phys. Rev. Lett. 89, 222002 (2002).

[7] R. Di Salvo, MENU2004, August 29th -Sep 4th 2004, Beijing, China.

[8] I. Jeaglé, NSTAR2005, 12 - 15 October 2005, Tallahassee, Florida USA.

[9] L. Tiator, NSTAR2005, 12 - 15 October 2005, Tallahassee, Florida USA.

[10] L. Tiator, MESON2006, 9 - 13 June 2006, Kraków, Poland.

[11] W.-T. Chiang, S.-N. Yang, L. Tiator, D. Drechsel, Nucl. Phys. A 700, 429 (2002).

[12] M.V. Polyakov and A. Rathke, Eur. Phy. J A18 691 (2003).

[13] O. Bartalini et al., Eur. Phys. J. A 26 399 (2006).

[14] V. Kouznetsov et al., Nucl. Instr. and Meth. A 487 396 (2002).

[15] V. Bartalini et al., Nucl. Instr. and Meth. A 562 85 (2006).